Author(s): SE, Krieger; C, Kim; L, Zhang; Marjomäki, Varpu; J, Bergelson

Title: Echovirus 1 entry into polarized Caco-2 cells depends on dynamin, cholesterol, and cellular factors associated with macropinocytosis

Year: 2013

Version:

Please cite the original version:

SE, K., C, K., L, Z., Marjomäki, V., & J, B. (2013). Echovirus 1 entry into polarized Caco-2 cells depends on dynamin, cholesterol, and cellular factors associated with macropinocytosis. Journal of Virology, 87(16), 8884-8895. https://doi.org/10.1128/JVI.03415-12

JVI Journals.ASM.org

Echovirus 1 Entry into Polarized Caco-2 Cells Depends on Dynamin, Cholesterol, and Cellular Factors Associated with Macropinocytosis

Sophie E. Krieger,[a] Chonsaeng Kim,[a] Lili Zhang,[a] Varpu Marjomaki,[b] Jeffrey M. Bergelson[a,c]

Division of Infectious Diseases, Children's Hospital of Philadelphia, Philadelphia, Pennsylvania, USA[a]; Department of Biological and Environmental Science/Nanoscience Center, University of Jyväskylä, Jyväskylä, Finland[b]; Department of Pediatrics, University of Pennsylvania Perelman School of Medicine, Philadelphia, Pennsylvania, USA[c]

Enteroviruses invade their hosts by crossing the intestinal epithelium. We have examined the mechanism by which echovirus 1 (EV1) enters polarized intestinal epithelial cells (Caco-2). Virus binds to VLA-2 on the apical cell surface and moves rapidly to early endosomes. Using inhibitory drugs, dominant negative mutants, and small interfering RNAs (siRNAs) to block specific endocytic pathways, we found that virus entry requires dynamin GTPase and membrane cholesterol but is independent of both clathrin- and caveolin-mediated endocytosis. Instead, infection requires factors commonly associated with macropinocytosis, including amiloride-sensitive Na^+/H^+ exchange, protein kinase C, and C-terminal-binding protein-1 (CtBP1); furthermore, EV1 accumulates rapidly in intracellular vesicles with dextran, a fluid-phase marker. These results suggest a role for macropinocytosis in the process by which EV1 enters polarized cells to initiate infection.

Echoviruses are common human pathogens that cause febrile illnesses, including many cases of viral meningitis (1). They are small nonenveloped viruses, grouped with coxsackieviruses and polioviruses in the *Enterovirus* genus of the family *Picornaviridae*. The picornavirus life cycle begins with attachment of the virus to a receptor on the cell surface, entry of the virus into the cell, and release of the single-strand, positive-sense RNA genome from the capsid into the cytoplasm, where translation and replication occur.

Picornaviruses bind to a variety of receptors (2) and use a variety of the cell's endocytic mechanisms for entry (3). The best-defined entry pathway is clathrin-mediated endocytosis, in which ligands and receptors are internalized in clathrin-coated vesicles. However, an increasing number of clathrin-independent mechanisms have also been identified; these are characterized by the involvement of the GTPase dynamin 2, cholesterol-rich membrane microdomains (lipid rafts), specific membrane-associated proteins such as caveolin or flotillin, or other specific cellular factors such as the small GTPase, Arf6 (4). A number of viruses have recently been shown to enter by mechanisms related to macropinocytosis (5), a process in which actin-based membrane ruffles, often produced in response to growth factor stimulation, fuse back to the plasma membrane, nonselectively trapping and internalizing large volumes of extracellular fluid (6). Macropinocytosis has often been distinguished from other endocytic mechanisms because of its sensitivity to amiloride (7); with increased understanding of the mechanisms by which membrane ruffling is regulated, macropinocytosis has been shown to involve a number of specific cellular factors, including protein and lipid kinases, Rho family GTPases, p21-activated kinase 1 (PAK1), and the PAK1 effector C-terminal-binding protein-1/brefeldin A–ADP-ribosylated substrate (CtBP1/BARS) (6).

Enteroviruses are transmitted by the oral-fecal route, and they initiate infection by crossing the intestinal mucosa, which is lined by polarized endothelial cells. We have now examined how the human pathogen echovirus 1 (EV1) (8) enters Caco-2 cells, a human colon cancer cell line that serves as an *in vitro* model of the intestinal epithelium (9). We find that EV1 binds its receptor, VLA-2, on the apical cell surface and then rapidly enters polarized Caco-2 cells by a mechanism that does not involve clathrin or caveolin but which instead shows many features characteristic of macropinocytosis.

MATERIALS AND METHODS

Cells and viruses. Caco-2 cells (ATCC HTB-37) were cultured in minimal essential medium with Earle's salts containing 20% fetal bovine serum, nonessential amino acids, sodium pyruvate, and penicillin-streptomycin. For infection assays and immunofluorescence microscopy, Caco-2 cells were plated in collagen-coated eight-well chamber slides (BD Biosciences) at a density of 4×10^4 cells/well and cultured for 2 days; under these conditions, cells show polarized localization of decay-accelerating factor (DAF; apical), coxsackievirus-adenovirus receptor (CAR) and zonula occludens 1 (ZO-1) (tight junction), and β-catenin (basolateral).

EV1 (Farouk strain) (10), EV7 (Wallace strain) (11), and coxsackievirus B3-RD variant (CVB3-RD) (12) were prepared, and titers were determined in HeLa cells as described previously (11). Vesicular stomatitis virus (VSV), provided by Ron Harty (University of Pennsylvania), was prepared, and titers were determined in BHK-21 cells as described previously (13).

Antibodies. For infection experiments with EV1, EV7, and CVB3-RD, cells were stained with a specific mouse monoclonal antibody against double-stranded RNA (dsRNA) (J2; English & Scientific Consulting, Hungary). Monoclonal antibody specific for VSV M protein (clone 23H12) was obtained from Douglas Lyles (Wake Forest University). Rabbit antiserum against purified EV1 has been described previously (14). For inhibition of EV1 binding and infection, we used a blocking anti-VLA-2 monoclonal antibody (AA10) (10) and an isotype-matched myeloma protein (MOPC-104E; Sigma) as a control.

For immunofluorescence, we used rabbit polyclonal anti-ZO-1 (ZO-1 N-term, 40-2300; Invitrogen), mouse monoclonal anti-VLA-2 (clone HAS3, catalog number MAB1233; R&D Systems), anti-endosomal anti-

Received 18 December 2012 **Accepted** 16 May 2013
Published ahead of print 5 June 2013
Address correspondence to Jeffrey M. Bergelson, bergelson@email.chop.edu.
S.E.K. and C.K. contributed equally to this article.

doi:10.1128/JVI.03415-12

gen 1 (EEA1) (BD 610457), mouse monoclonal anti-LAMP-2 (clone H4B4; Developmental Studies Hybridoma Bank, University of Iowa), and goat secondary antibodies conjugated to fluorescein isothiocyanate (FITC) (Jackson ImmunoResearch, West Grove, PA) or Alexa Fluor-488, -594, or -633 (Invitrogen, Carlsbad, CA).

For immunoblotting, we used mouse anti-clathrin heavy chain (CHC) (catalog number 610499; BD Transduction Laboratories [BD], San Jose, CA), rabbit anti-caveolin (610060; BD), mouse anti-CtBP1 (612042; BD), rabbit anti-dynamin 2 (ab3457; Abcam, Cambridge, MA), rabbit polyclonal anti-Rab5 (KAP-GP006; Stressgen), and rabbit polyclonal anti-Rab7 (R4479; Sigma). Horseradish peroxidase (HRP)-conjugated glyceraldehyde-3-phosphate dehydrogenase (GAPDH) antibody (sc-25778) and secondary antibodies conjugated to horseradish peroxidase were purchased from Santa Cruz Biotechnology.

Chemical inhibitors. For experiments with most inhibitory drugs, Caco-2 cells were pretreated for 45 min, and drug was present during virus binding and infection. Chlorpromazine (CPZ) (10 to 20 μg/ml), filipin III (1 to 2 μg/ml), 5-(*N*-ethyl-*N*-isopropyl) amiloride (EIPA) (50 μM), and cytochalasin D (10 μg/ml) were obtained from Sigma (St. Louis, MO). Dynasore (80 to 120 μM), bafilomycin A1 (10 nM), and rottlerin (1 μM) were obtained from Calbiochem (San Diego, CA). Jasplakinolide (1 μM) was purchased from Invitrogen. The PAK1 inhibitor IPA-3 (20 μM) and its inactive analogue PIR3.5 (20 μM) were obtained from Calbiochem (San Diego, CA) and Tocris Bioscience (Bristol, United Kingdom), respectively. For experiments with methyl-beta-cyclodextrin (MβCD), a fast-acting drug that extracts cholesterol from the plasma membrane, cells were exposed according to two schedules: either cells were pretreated with MβCD (5 to 10 mM; Sigma) for 45 min with no drug present during virus binding and infection, or MβCD was added for a period of 45 min, beginning at 2 h postinfection (p.i.). In experiments with MβCD where cholesterol was added back, MβCD-treated cells were exposed to 0.5 mM water-soluble cholesterol (Sigma) with 10 mM MβCD. For dynasore and lipid raft disruption experiments, we used complete medium with 20% NuSerum (BD Biosciences, Bedford, MA) in place of fetal bovine serum (FBS) because serum components can decrease the efficacy of those drugs.

In some experiments, cells were treated with drugs either early or late in infection. To test early effects, drugs were present during a preincubation period of 45 min, during a virus binding period of 45 min, and during the first 2 h of infection (a total of 3.5 h); then drug was removed, and cells were incubated with drug-free medium. To test late effects, virus was bound to untreated cells, infection was initiated at 37°C, and drug-containing medium was added at 2 h postinfection (for a period of 3.5 h). In both cases, infection was measured at 5.5 h postinfection.

Paracellular permeability. Transepithelial resistance (RT) measurements were performed with an ohmmeter (EVOM; World Precision Instruments, Sarasota, FL) on cells grown on 12-mm Transwell filters (0.4-μm pore size; Costar) for 2 days.

Plasmids and small interfering RNAs (siRNAs). Plasmids encoding green fluorescent protein (GFP)-tagged wild-type (WT) and K44A dominant negative (DN) dynamin 2 (15) were provided by Mark McNiven (Mayo Institute, Rochester, MN); GFP-tagged WT and Y14F DN caveolin (16) were from Ari Helenius (Swiss Federal Institute of Technology, Zurich); EPS15-GFP WT and DN (17) were provided by Alice Dautry-Varsat (Institut Pasteur, Paris). GFP-tagged WT and DN (S34N) Rab5 were provided by George Bloom (University of Virginia), and WT and DN (T22N) Rab7 were provided by Craig Roy (Yale University). CtBP1 WT, CtBP1 with the mutation S157A (CtBP1-S157A; dominant negative), and CtBP1-S147D (constitutively active) (18) were provided by Urs Greber (University of Zurich). Caco-2 cells (5×10^5) were transfected with 5 to 10 μg of plasmids using an Amaxa Nucleofector System (Lonza). Transfected cells were divided among four wells in a collagen-coated eight-chamber slide (BD) and used for virus infection 2 days later.

Pooled validated siRNAs targeting dynamin 2 (M-004007-03), clathrin heavy chain (M-004001-00), and Cav-1 (M-003467-01) were purchased from Dharmacon (Chicago, IL). Pooled siRNAs targeting Rab5 a, b, and c isoforms have been described previously (11). CtBP1 siRNAs (siRNA 1, 5′-CCG UCA AGC AGA UGA GAC A-3′; siRNA 2, 5′-GGA UAG AGA CCA CGC CAG U-3′) were synthesized based on sequences reported in Amstutz et al. (18). Rab7 siRNA (sc-29460) was purchased from Santa Cruz. Control siRNA has been described previously (19). Cells were transfected with 20 nM siRNA in six-well plates using Lipofectamine 2000 (Invitrogen) according to the manufacturer's protocol. After 24 h, the monolayers were trypsinized, cells were replated at 4×10^4 cells/well in collagen-coated eight-well chamber slides, and infections were performed 2 days later. Depletion of targeted proteins was confirmed by immunoblot analysis of parallel samples.

Binding assays. EV1 was radiolabeled with [^{35}S]methionine-cysteine mixture as described previously (10). ^{35}S-labeled virus (20,000 cpm per well) was bound to confluent Caco-2 cells in 24-well plates for 1 h at room temperature. Unbound virus was removed with three washes with phosphate-buffered saline (PBS), cells were lysed with Solvable detergent (PerkinElmer, Waltham, MA), and cell-bound radioactivity was assessed.

Virus infection and entry assays. For both infection and entry experiments, cells were plated on eight-well chamber slides coated with collagen (BD Biosciences) at 4×10^4 cells/well. Virus in binding buffer (minimal essential medium with 20 mM HEPES) was allowed to bind to cells for 1 h at 4°C. Unbound virus was washed off, complete medium was added, and cells were placed at 37°C to initiate infection or virion entry. Infection experiments were ended at 6 h with fixation and permeabilization with a 3:1 mixture of ice-cold methanol-acetone. For measurements of infection, cells were stained with an anti-dsRNA antibody (clone J2) for 1 h at a 1:500 dilution in PBS. After three short washes, secondary antibody was added for 45 min at a 1:500 dilution with 10% normal serum from the same source as the secondary antibody. Images were captured with an Olympus BX51 immunofluorescence microscope, using a 20× objective. Three or four fields (700 to 1,000 cells) were captured for each monolayer. The number of infected cells and the total number of nuclei stained with 4′,6′-diamidino-2-phenylindole (DAPI) were quantified using ImageJ software (http://rsbweb.nih.gov/ij/).

For entry experiments with EEA1 colocalization, cells were fixed with methanol-acetone and stained with anti-EV1 rabbit antibody and anti-EEA1 mouse antibody and with anti-rabbit and anti-mouse secondary antibodies conjugated to Alexa Fluor-488, -594, or -633. In some experiments, to determine whether virus had been internalized from the cell surface, cells were fixed with 4% paraformaldehyde and stained with anti-EV1 antibody and Texas Red-labeled secondary antibody before permeabilization to detect virus on the cell surface; then, to detect internalized virus, cells were fixed again with 4% paraformaldehyde, permeabilized with 0.1% Triton X-100 in PBS, and restained with anti-EV1 antibody and FITC-conjugated secondary antibody. Slides were mounted with Vectaschield (Vector Laboratories). Entry images were captured using a Leica TCS 4D laser scanning confocal microscope using a 63× oil objective. For three-dimensional analysis, XZ- or YZ-series stacks were acquired at 0.4-μm intervals and viewed with the LSM Reader plug-in for ImageJ.

For experiments with VSV, 1 PFU/cell was allowed to bind to cells for 1 h at 37°C, unbound virus was removed, complete medium was added, and virus was allowed to infect cells for 5 h. Infected cells were detected with anti-M protein antibody (clone 23H12).

Transferrin and dextran uptake assay. For all transferrin uptake experiments, cells were serum starved for 30 min prior to the start of the experiment. Cells were incubated with 10 μg/ml transferrin conjugated to Alexa Fluor-594 for 40 min at 37°C. Following the entry period, surface transferrin was stripped with two 5-min acid washes (0.2 N acetic acid, 0.5 M NaCl, pH 2.5) at 4°C. Chambers were removed, and slides were submerged 10 times in ice-cold PBS and mounted using Vectashield. For quantification, four fields using a 20× objective were captured per well, and cells were scored for internalized transferrin based on the Alexa Fluor-594 signal (400 to 600 total cells).

Dextran (70 kDa) conjugated to Texas Red (lysine fixable; Invitrogen) was used at 1 mg/ml. After 45 min of binding at 4°C, virus was removed by

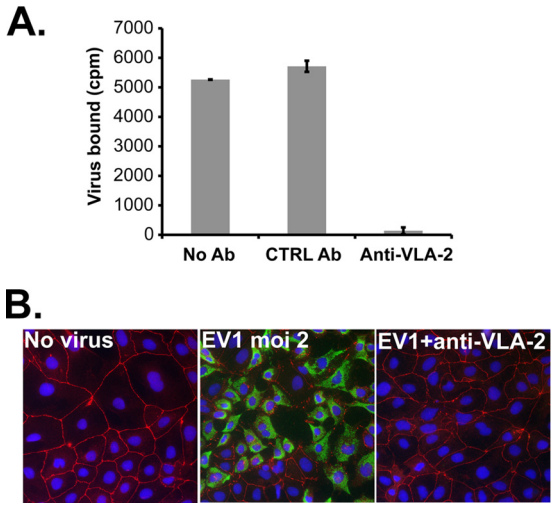

FIG 1 EV1 binds to VLA-2 on Caco-2 cells. (A) Virus binding. ^{35}S-labeled EV1 (20,000 cpm) was incubated with polarized Caco-2 cells pretreated with medium alone (No Ab), with control antibody (CTRL Ab), or with anti-VLA-2 antibody. Results are shown as mean virus bound ± SD for triplicate samples. (B) Infection. Caco-2 cells were preincubated with control or anti-VLA-2 antibody for 45 min at 37°C. Cells were then exposed to EV1 (MOI of 2) and incubated for 6 h at 37°C to allow infection to proceed. Infection was detected by staining with antibody specific for double-stranded RNA (green). Cells were also stained with an anti-ZO-1 antibody (red).

washing with PBS, and dextran, diluted in medium with 0.1% bovine serum albumin (BSA), was added to the cells for 10 or 30 min. Cells were then washed four times with PBS and fixed with a 3:1 mixture of ice-cold methanol-acetone.

Colocalization with endosomal markers. Caco-2 monolayers were incubated with EV1 at 37°C. At the times indicated in Fig. 7, monolayers were fixed with a 3:1 mixture of ice-cold methanol-acetone and stained with antibodies specific for EV1 and EEA1 or LAMP-2 and examined by confocal microscopy. Images with the best focus in the green (virus) channel were captured and analyzed. Colocalization of red and green signal was determined, using the Colocalization Test plug-in in the Wright Cell Imaging Facility (WCIF) ImageJ bundle to calculate Pearson's correlation coefficient for each cell. Three independent experiments were performed. In each experiment, 100 to 160 cells were analyzed for each time point.

Statistical analysis. Student's *t* test was used to determine statistical significance. In all graphs, results are indicated as the means and standard deviations (SD) of at least three samples.

RESULTS

EV1 infects polarized Caco-2 cells by binding to VLA-2 on the apical cell surface. The identified EV1 receptor is VLA-2, the α2β1 integrin (10), which functions in cell adhesion to extracellular matrix components (20) and which might thus be expected to localize to the basolateral surface of intestinal epithelium. We were therefore interested to learn whether EV1 uses VLA-2 to infect polarized Caco-2 cells. ^{35}S-labeled EV1 bound to the apical surface of polarized Caco-2 monolayers (Fig. 1A), and binding was inhibited specifically by an anti-VLA-2 monoclonal antibody (AA10) previously shown to inhibit virus interaction with VLA-2 (10). When monolayers were exposed to EV1 at a low multiplicity of infection (MOI of 2 PFU/cell), infection was evident by 6 h, as detected by staining with antibody specific for double-stranded RNA (dsRNA) (Fig. 1B). No dsRNA staining was observed in monolayers not exposed to virus, and no staining was observed in virus-exposed monolayers pretreated with the VLA-2 antibody. These results indicate that infection from the apical surface depends on virus attachment to VLA-2.

These experiments were performed with Caco-2 cells grown on collagen-coated tissue culture wells. Such cells are morphologically polarized, as demonstrated by the discrete localization of apical, basolateral, and tight junction marker proteins, and they have been used for previous studies of virus entry (12, 21). However, it is not possible to measure the functional integrity of their tight junctions. We therefore cultured Caco-2 monolayers on transwell membranes until the transepithelial electrical resistance, a measure of junctional integrity, was greater than 1,000 Ω-cm^2. These monolayers were readily infected by virus added to the apical transwell chamber, confirming that EV1 infects polarized Caco-2 cells by directly accessing VLA-2 receptors on the apical surface rather than by passing through junctions to reach the basolateral side (data not shown).

EV1 enters cells with VLA-2 and moves to early endosomes. To examine the entry of virus particles into the cells, we permitted EV1 to bind to monolayers in the cold (MOI of 200), washed off unbound virus, and then permitted infection to proceed at 37°C. At intervals, cells were fixed, permeabilized, and stained to detect both virus and VLA-2 (Fig. 2A). At 0 min, virus was evident as small speckles on the cell surface; VLA-2 appeared to be present both on the cell surface and within the cell. At 5 min, virus and VLA-2 colocalized in clusters; these clusters were detected even when cells were not permeabilized before staining (data not shown), indicating that they were present on the cell surface rather than within the cell. By 20 min both virus and VLA-2 were concentrated in vesicles surrounding the cell nucleus, where they persisted until at least 40 min. These results suggest that, after binding to VLA-2, virus clusters with VLA-2 on the cell surface and then moves with VLA-2 to perinuclear vesicles within the cell. Colocalization of virus and early endosomal antigen 1 (EEA1) indicated that many of these vesicles are early endosomes (Fig. 2B).

Dynamin and cholesterol are required for EV1 infection. Dynamin 2, a large GTPase involved in pinching off endocytic vesicles, is important for a variety of endocytic pathways, including both clathrin- and caveolin-mediated entry (4). We found that depletion of dynamin with siRNA inhibited infection by EV1 (Fig. 3A); as expected, dynamin depletion also inhibited transferrin uptake (13) but had no effect on infection by CVB3 (11). EV1 infection was also inhibited in cells expressing a dominant negative form of dynamin (Fig. 3B, K44A). Dynasore, a reversible inhibitor of dynamin 2 function (22), inhibited infection by EV1 (Fig. 3C) and, as previously reported (11), inhibited EV7 infection and transferrin uptake but had no effect on infection by CVB3. To determine whether dynamin was important primarily for early events or late events in infection, we measured the effects of dynasore present at early (from −1.5 to 2 h) or late (from 2 to 5.5 h) times postinfection (Fig. 3D); the predominant effect was seen when dynasore was present early during infection. These results indicate that dynamin is required for EV1 infection in these cells and that it is primarily important for events that occur within the first 2 h.

Membrane cholesterol is important both for endocytosis in caveolae and for other noncaveolar mechanisms of virus entry (4). Depletion of cholesterol with methyl-β-cyclodextrin (MβCD) inhibited EV1 infection, and the inhibition was reversed when cells were supplied with cholesterol (Fig. 4A). As previously observed

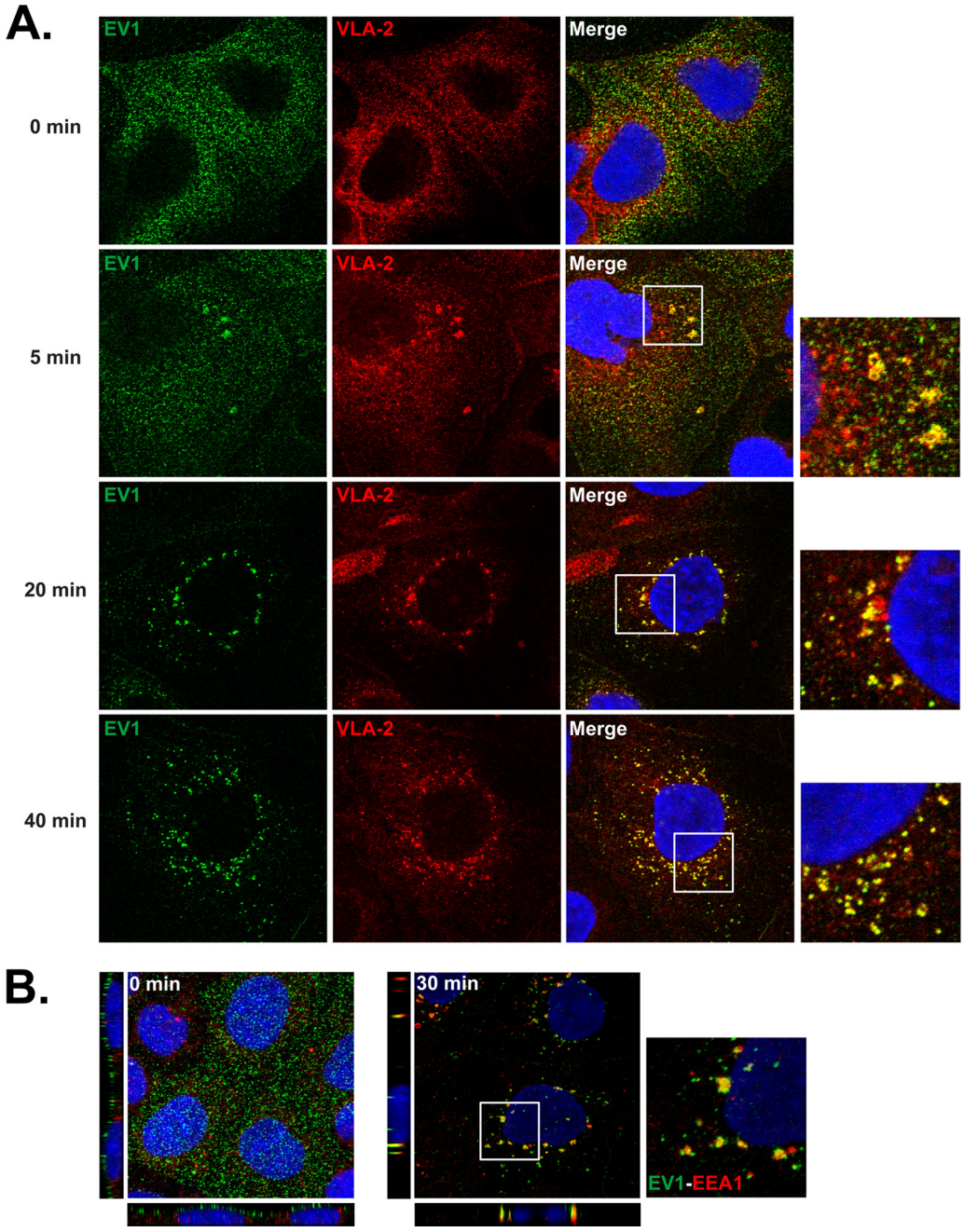

FIG 2 EV1 enters the cell with VLA-2 and moves to early endosomes. (A) Colocalization with VLA-2. Cells were exposed to EV1 (MOI of 200) in the cold and then incubated at 37°C to permit entry to occur. At the indicated times, cells were fixed and stained with anti-EV1 (green) and anti-VLA-2 (red) antibodies. (B) Colocalization with EEA1. Cells exposed to EV1 were incubated for 0 or 30 min at 37°C and then stained to detect virus (green) and EEA1 (red). XZ and YZ projections are shown at left and below.

(11), MβCD had no effect on infection by EV7, which enters by clathrin-mediated endocytosis. MβCD inhibited EV1 infection when it was added early but not when it was added at 2 h p.i. (late, Fig. 4B).

Filipin is a drug that binds to cholesterol, disrupts caveolae, perturbs the structure of lipid rafts, and interferes with many raft-dependent cellular processes but does not remove cholesterol from cellular membranes (23, 24). We saw no effect of filipin on EV1 infection at a concentration that, as we previously observed (12), was sufficient to inhibit infection by CVB3 (Fig. 4B). These results indicate that membrane cholesterol is important for some cellular function required for EV1 infection, although that function is relatively insensitive to filipin. Other investigators have also reported divergent effects of MβCD and filipin on raft-dependent endocytic and signaling functions (25–27).

Dynamin and cholesterol are important for EV1 entry. To determine whether dynamin and cholesterol were specifically required for virus entry (as opposed to other events in the virus life

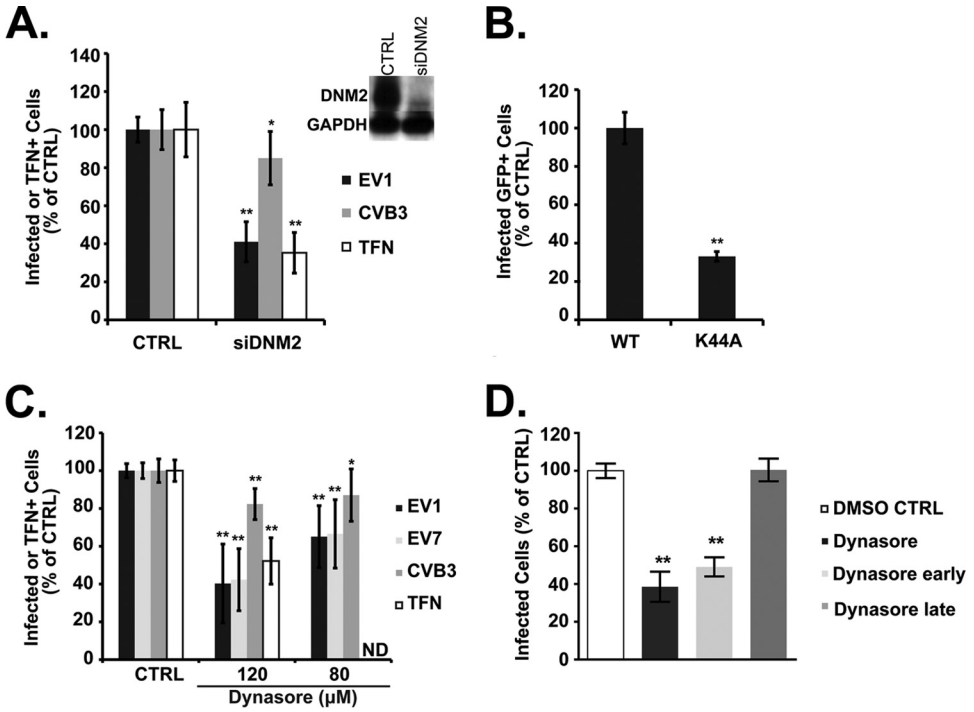

FIG 3 EV1 infection requires dynamin. (A) Caco-2 cells transfected with siRNA targeting dynamin 2 (siDNM2) were infected with EV1 or CVB3 or incubated with Alexa Fluor-594-labeled transferrin (TFN), and infection and transferrin uptake were measured as described in Materials and Methods. Depletion of dynamin (DNM2) was confirmed by immunoblotting (inset). (B) Caco-2 cells transfected with plasmids expressing GFP-labeled wild-type dynamin 2 or dominant negative dynamin 2 (K44A) were infected with EV1. Infection of transgene-expressing cells (GFP-positive) was determined by staining for dsRNA and normalized to results in control cells expressing the WT. (C) Caco-2 cells were pretreated with dynasore at a concentration of 80 or 120 μM before exposure to EV1, EV7, CVB3, or transferrin (TFN), and cells were incubated in the presence of dynasore throughout infection. (D) Cells were treated with 120 μM dynasore throughout infection (−1.5 h to 5.5 h, dynasore), early in infection (−1.5 h through 2 h p.i., dynasore early), or late in infection (2 h to 5.5 h, dynasore late), as described in Materials and Methods. In all graphs, results are shown as the mean number of infected or TFN-containing cells, normalized to the results in control cells (±SD) for triplicate samples from each of three or four independent experiments. TFN uptake was not measured in the presence of 80 μM dynasore (ND). DMSO, dimethyl sulfoxide. *, $P < 0.05$; **, $P < 0.01$.

cycle), we examined the colocalization of virus and EEA1 at 30 min after infection in cells that had been treated with dynasore or MβCD. Although some virus colocalized with EEA1 in dynasore-treated cells (Fig. 5B), most virus remained on the cell surface, in contrast to what was observed in control cells (Fig. 5A). In cells exposed to MβCD (Fig. 5C), virus appeared trapped on the cell surface, and little or no colocalization was seen with EEA1 inside the cell. To confirm that virus was retained on the cell surface, we used a two-color staining technique in which unpermeabilized cells were stained with anti-EV1 antibody and red-conjugated secondary antibody to detect virus on the surface; cells were then permeabilized to expose intracellular virus and restained with anti-EV1 and green-conjugated secondary antibody. In merged images, internalized virus appears green, and virus on the cell surface appears either yellow or red. In control cells, green perinuclear staining was evident (Fig. 5D). In cells treated with dynasore, green perinuclear staining was much less evident, with most cells showing virus retained on the cell surface (Fig. 5E). After MβCD treatment, although green staining was still seen in some cells (Fig. 5F, arrow), virus was retained on the surface of many cells (inset). Taken together, the results with dynasore and MβCD indicate that dynamin and cholesterol are important for virus entry into cells.

EV1 infection does not require caveolin or clathrin. Caveolar endocytosis depends on cholesterol and dynamin, but its most characteristic feature is a requirement for functional caveolin 1. We saw no inhibition of EV1 infection when caveolin 1 was depleted with a specific siRNA (Fig. 6A) or when its function was inhibited by expression of a dominant negative mutant (Fig. 6B, Y14F); however, in control experiments, CVB3 infection was seen, as expected (11, 12), to depend on caveolin. These results indicate that EV1 infection and entry do not require caveolin.

To test the role of the clathrin-mediated pathway, we depleted cells of clathrin heavy chain, inhibited the function of the clathrin adaptor protein Eps15, and treated cells with chlorpromazine (CPZ), a drug that is commonly used to block clathrin-mediated endocytosis (4). Depletion of clathrin heavy chain (CHC) with siRNA markedly inhibited transferrin uptake, which is known to depend on clathrin, but had only a small (although statistically significant) effect on EV1 infection (Fig. 6C). Similarly, a dominant negative mutant of the clathrin adaptor protein Eps15 inhibited infection by vesicular stomatitis virus (VSV), which depends on the clathrin pathway for entry (28, 29), and had a statistically significant but smaller effect on infection by EV1 (Fig. 6D). These results suggested a possible role for clathrin in EV1 infection. However, CPZ had no effect on EV1 infection (Fig. 6E) at concentrations that showed marked inhibitory effects on infection by two clathrin-dependent viruses, EV7 (11) and VSV (28, 29). These results suggest that, although clathrin-dependent processes may

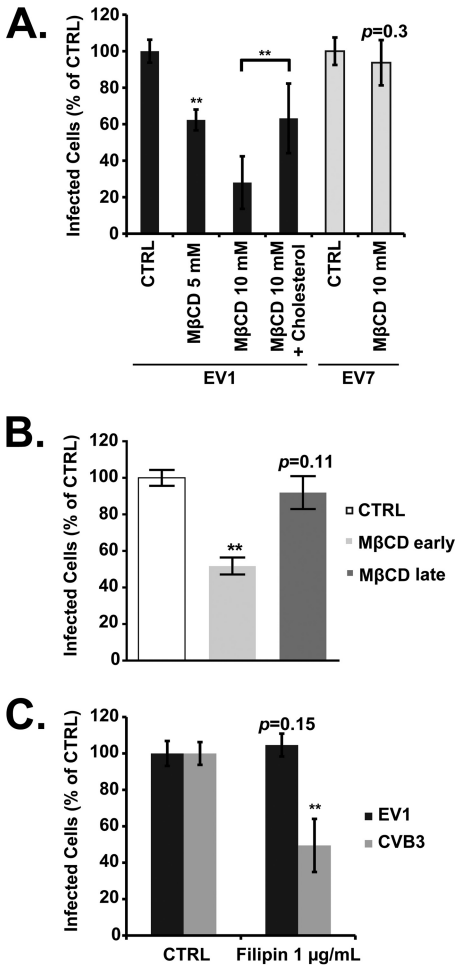

FIG 4 EV1 infection requires cholesterol. (A) Caco-2 cells were pretreated with MβCD or MβCD plus cholesterol before infection with EV1, EV7, or CVB3. (B) Cells were pretreated with MβCD before exposure to EV7 (early) or at 2 h postinfection (late). (C) Cells were pretreated with filipin before infection with EV1, EV7, or CVB3. Means ± SD of three independent experiments performed in triplicate are shown. **, $P < 0.01$.

play some role in EV1 infection, clathrin-mediated endocytosis is not the major route by which EV1 enters the cell.

Rab5, but not Rab7, is needed for EV1 infection. As shown above (Fig. 2B), we detected EV1 in early endosomes within 30 min after infection. To gain a better sense of how EV1 moves within the endosomal system, we quantified the colocalization of virus with the early endosomal marker EEA1 (Fig. 7A) and the late endosomal marker LAMP-2 (Fig. 7B) at intervals after infection. Colocalization with EEA1 was maximal at 20 to 40 min and then decreased, whereas colocalization with LAMP-2 was less striking and increased slowly for at least 120 min. These results suggest that EV1 is delivered first to early endosomes and then, much later, to late endosomes.

Two small GTPases, Rab5 and Rab7, are critical for vesicular traffic through the endosomal system: Rab5 controls the delivery of cargoes to the early endosome, whereas Rab7 is important for maturation of late endosomes (30). Infection was inhibited by siRNA targeting Rab5 (Fig. 7C) and by expression of dominant negative Rab5 (Fig. 7D); in contrast, Rab7 siRNA had only a slight inhibitory effect (Fig. 7C), and dominant negative Rab7 (Fig. 7E) had no inhibitory effect on EV1 infection. Bafilomycin A, which prevents endosomal acidification by inhibiting the vacuolar proton pump, blocked infection by VSV, a virus that is known to require endosomal acidification for fusion and entry (31), but had only a slight effect on infection by EV1 (Fig. 7F). These results suggest that infection depends on virus delivery to early endosomes but that maturation of late endosomes and endosomal acidification are not essential for EV1 entry.

Factors implicated in macropinocytosis are important for EV1 infection and entry. Previous studies showed that, in some nonpolarized cells, EV1 infection involves factors important for macropinocytosis, a process by which cells engulf extracellular fluid. Agents that perturb actin polymerization, Na^+/H^+ exchange, p21-activated kinase (PAK1) activity, or the activity of protein kinase C (PKC), are all known to inhibit macropinocytosis (5), and all inhibit infection by EV1 in osteosarcoma cells engineered to express VLA-2 (32); further, EV1 infection in these cells requires C-terminal binding protein 1/brefeldin A–ADP-ribosylated substrate (CtBP1/BARS), a PAK1 effector involved in macropinosome internalization (33). In Caco-2 cells, entry of CVB3 is also known to involve macropinocytosis (21). We therefore examined whether selected inhibitors of macropinocytosis affected EV1 infection and entry into Caco-2 cells.

EV1 infection (like infection by CVB3) was inhibited by the amiloride derivative EIPA, an inhibitor of Na^+/H^+ exchange (Fig. 8A), by cytochalasin D and jasplakinolide, which perturb actin dynamics by different mechanisms (Fig. 8B), by rottlerin, an inhibitor of PKC (Fig. 8C), and by the PAK inhibitor IPA-3 but not by its inactive derivative PIR3.5 (Fig. 8D). In a control experiment (data not shown) rottlerin markedly inhibited uptake of fluorescently labeled dextran, a fluid-phase marker commonly used to measure macropinocytosis, but did not inhibit internalization of transferrin.

CtBP1/BARS is a PAK1 substrate required for the closure of macropinosomes and their fission from the plasma membrane (33). To test the role of CtBP1 in EV1 infection, we used two CtBP1 siRNAs previously shown to inhibit fluid-phase uptake in HeLa cells (18). Although moderate depletion of CtBP1 protein was achieved with both siRNAs, one siRNA had a marked inhibitory effect on infection, whereas the other had only a small (although statistically significant) effect (Fig. 8E). Because of these inconsistent results, we also tested the effects of CtBP1 mutants (Fig. 8F). CtBP1-S147A is not susceptible to phosphorylation by PAK1 and has a dominant negative effect on macropinocytosis (18); in contrast, the phosphomimetic mutant S147D functions normally. When expressed in Caco-2 cells, S147A inhibited EV1 infection, whereas S147D did not, supporting the idea that CtBP1 is important for EV1 infection.

To determine whether inhibitors of macropinocytosis blocked early events or later events in infection, we treated cells with EIPA, cytochalasin D, rottlerin, and IPA-3 before 2 h or after 2 h postinfection. Cytochalasin D (Fig. 8H) and rottlerin (Fig. 8I) inhibited infection only when added early, and EIPA had a greater effect when added early than when it was added late (Fig. 8G). However, IPA-3 had a more pronounced effect when added after 2 h, suggesting that it acts predominantly on postentry events in infection (Fig. 8J).

In cells exposed to EIPA and cytochalasin D, virus internalization was inhibited, with virus almost fully retained on the cell

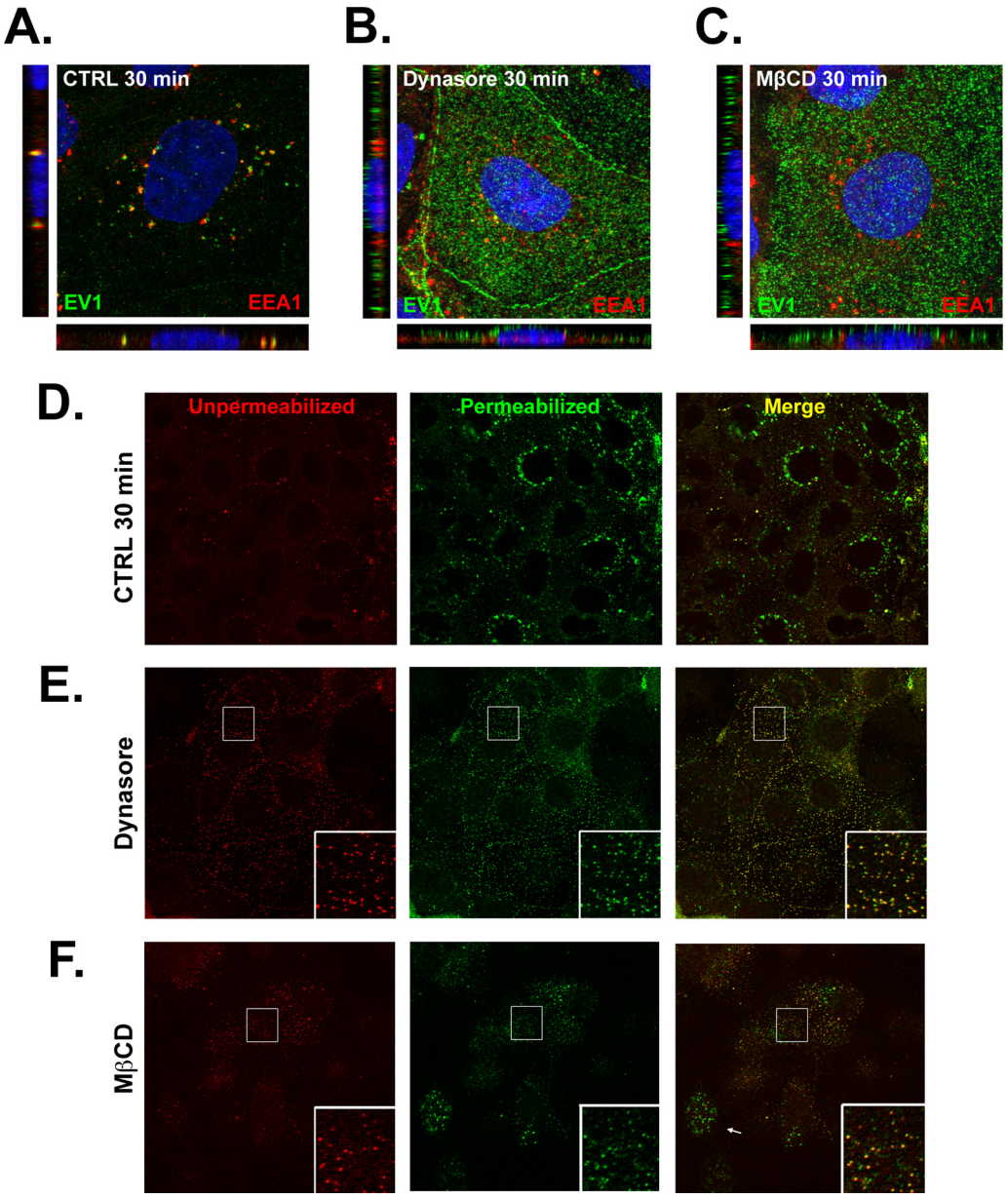

FIG 5 EV1 entry depends on dynamin and cholesterol. In panels A to C, Caco-2 cells were exposed to EV1 for 30 min at 37°C, fixed, permeabilized, and stained to detect EV1 (green) and EEA1 (red). (A) Control cells were pretreated with dimethyl sulfoxide vehicle alone. (B) Cells treated with 120 μM dynasore. (C) Cells treated with 10 mM MβCD. In panels D to F, cells were fixed at 30 min p.i. and stained with anti-EV1 and red-conjugated secondary antibody; cells were then permeabilized and restained with anti-EV1 antibody and green-conjugated secondary antibody. (D) Control cells were pretreated with dimethyl sulfoxide vehicle alone. (E) Cells were treated with 120 μM dynasore. In each frame, the boxed area is expanded in the lower right corner. (F) Cells treated with 10 mM MβCD. In panel F, the arrow indicates a cell with internalized virus. In each frame, the boxed area is expanded in the lower right corner.

surface at 30 min postinfection (Fig. 9; compare to untreated cells in 5A and D); in cells exposed to rottlerin, virus internalization was also largely inhibited although internalized virus was seen in some cells (Fig. 9B, arrow). These results indicate that virus entry by EV1 is inhibited by EIPA, cytochalasin D, and rottlerin and thus depends on a number of cellular factors involved in macropinocytosis. In cells treated with IPA-3, although some virus was retained on the cell surface, internalized virus was seen in many cells, scattered through the cytoplasm rather than concentrated in perinuclear vesicles. It is thus possible that IPA-3 inhibits infection by interfering with virus trafficking or other later events in the virus life cycle.

If EV1 is internalized in macropinosomes, we would expect virus to colocalize with dextran during the entry process. To examine this, we allowed virus to attach to cells in the cold, added dextran, and then raised the temperature to 37° to permit virus entry and dextran uptake. By 30 min postinfection, virus and dextran were observed together in perinuclear vesicles, identified as early endosomes by costaining with EEA1 (Fig. 10). At 10 min virus and dextran were also seen together in more peripheral ves-

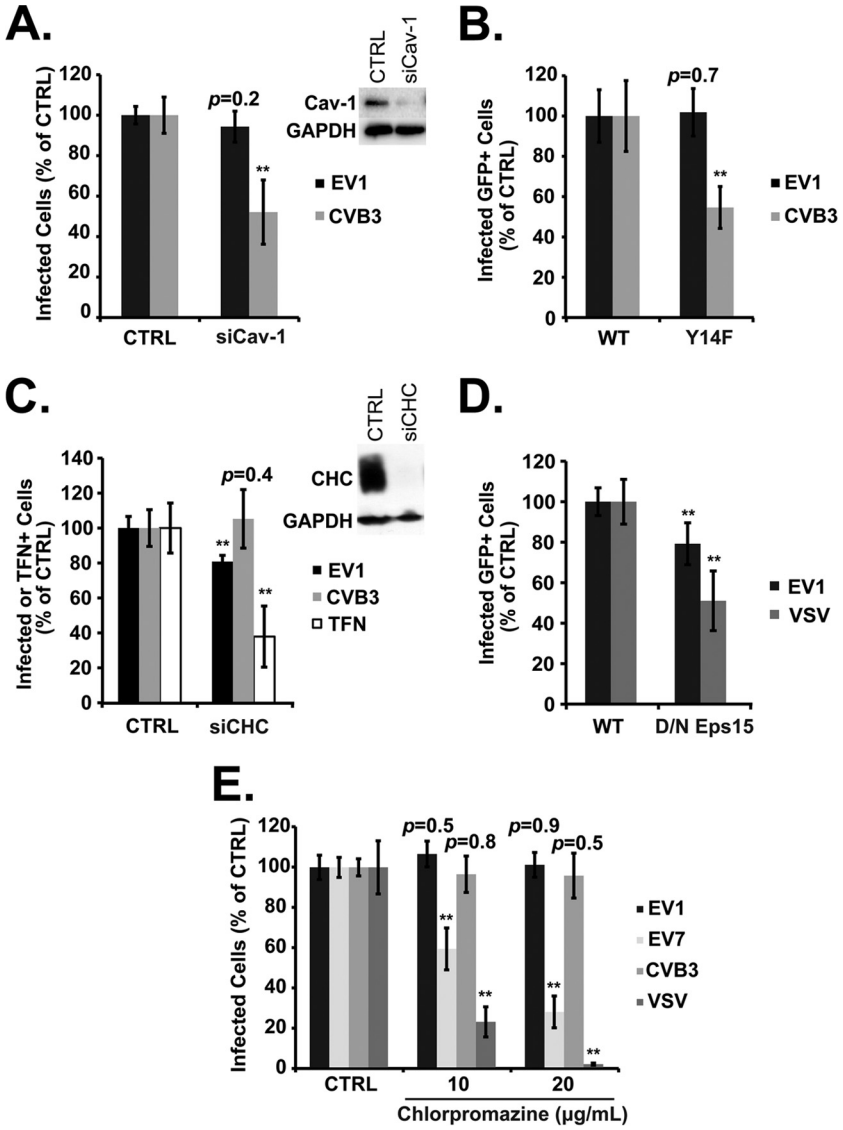

FIG 6 EV1 infection does not depend on caveolin- or clathrin-mediated endocytosis. (A) Caco-2 cells transfected with siRNA targeting caveolin-1 (siCav-1) were infected with EV1 or CVB3. (B) Caco-2 cells transfected with plasmids expressing GFP-tagged wild-type caveolin 1 (WT) or a dominant negative form (Y14F) were infected with EV1 or CVB3; results for Y14F cells were normalized to those obtained for control cells expressing the WT. (C) Caco-2 cells transfected with siRNA targeting clathrin heavy chain (siCHC) were infected with EV1 or CVB3 or incubated with labeled transferrin (TFN). (D) Caco-2 cells transfected with plasmids expressing GFP-tagged wild type (WT) or dominant negative (DN) Eps15 were infected with EV1 or VSV; results for DN cells were normalized to those obtained for control cells expressing the WT. (E) Caco-2 cells were pretreated with 10 to 20 μg/ml of chlorpromazine before infection with EV1 (MOI of 2), EV7 (MOI of 2), CVB3 (MOI of 3), or VSV (MOI of 2). In all graphs, means ± SD of at least three independent experiments performed in triplicate are shown. **, $P < 0.01$.

icles, some of which showed little or no staining with EEA1 antibody. These results suggest that virus and dextran traffic together before they are delivered to perinuclear early endosomes.

DISCUSSION

The results we report here indicate that EV1, after binding to VLA-2 on the apical surface of polarized epithelial cells, rapidly enters the cell and moves with VLA-2 to early endosomes. Virus entry is independent of both clathrin- and caveolin-mediated endocytosis but requires dynamin GTPase and membrane cholesterol. Further, we found that virus internalization and infection were inhibited by a variety of agents that disrupt macropinocytosis, suggesting a role for macropinocytosis in the entry process.

Macropinocytosis is a process in which cells use actin-based membrane protrusions to capture and internalize extracellular fluid into vacuoles of variable size. A growing number of viruses have been found to enter cells by mechanisms that involve macropinocytosis (reviewed in reference 5): in some cases, virus is taken up directly in macropinosomes; in others, activation of macropinocytosis may facilitate entry in some other way. We found that EV1 internalization into Caco-2 cells was inhibited by EIPA and rottlerin, two agents classically used to prevent macropinocytosis (7, 34), as well as by disruption of actin polymeriza-

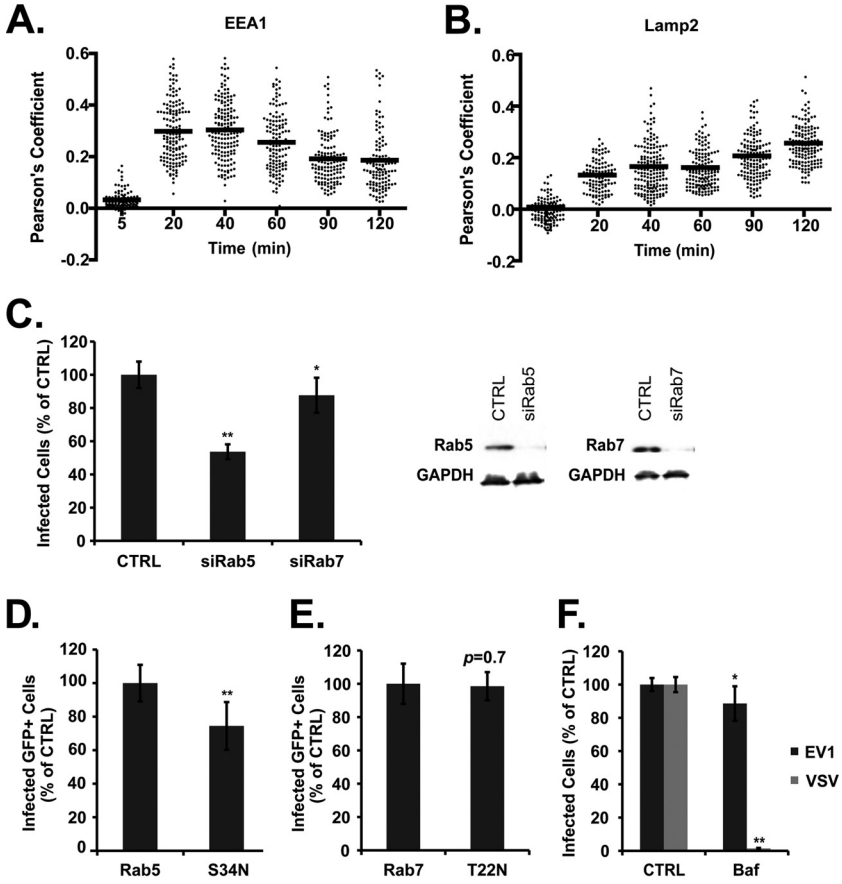

FIG 7 EV1 infection requires Rab5 but not Rab7. (A) Colocalization between intracellular virus and EEA1, expressed as Pearson's coefficient, measured for individual cells, with mean values shown. (B) Colocalization between intracellular virus and LAMP-2, expressed as Pearson's coefficient, measured for individual cells, with mean values shown. (C) Cells transfected with siRNAs targeting Rab5 (siRab5) or Rab7 (siRab7) were infected with EV1. Immunoblot shows silencing of Rab5 and Rab7 (right). Cells were transfected with plasmids expressing GFP-tagged wild-type Rab5 or dominant negative Rab5 (S34N) (D) or wild-type or dominant negative Rab7 (T22N) (E) and then infected with EV1. Infection of transgene-expressing cells (GFP-positive) was determined by staining for dsRNA; results for cells expressing dominant negative mutants were normalized to those obtained for control cells expressing the WT. (F) Cells pretreated with bafilomycin A1 (Baf; 1 μM) before exposure to EV1 or VSV. Means ± SD of at least three independent experiments performed in triplicate are shown. *, $P < 0.05$; **, $P < 0.01$.

tion. Infection was also blocked by inhibition of PAK1, which regulates macropinocytosis by phosphorylating CtBP1/BARS (18, 33), by depletion of CtBP1 with siRNA, and by expression of dominant negative CtBP1. However, the PAK1 inhibitor IPA-3 blocked infection even when it was added at 2 h, when virus internalization had already occurred, and did not appear to prevent internalization as effectively as dynasore, rottlerin, EIPA, or cytochalasin D. Thus, although we cannot exclude a possible role for PAK1 in virus entry, our results suggest that it is more important for postentry events than it is for virus internalization *per se*.

We found that virus colocalized with dextran, a marker of the macropinocytotic pathway, within 10 min (that is, before delivery to early endosomes). This would be expected if virus were taken up in macropinosomes. However, because we have not visualized the precise moment when virions enter the cell, we cannot exclude the possibility that virus is initially internalized by another mechanism and meets dextran within the endocytic system after entry has occurred.

We previously examined the entry of two other picornaviruses into polarized Caco-2 cells. EV7 binds to decay-accelerating factor (DAF) on the apical surface and then is internalized by clathrin-mediated endocytosis (11). CVB3 also binds to DAF, but it moves to the tight junction before entering the cell by a process that involves cholesterol and caveolin, but not dynamin (12). CVB3 entry from the tight junction is accompanied by a loss of junctional integrity and appears to require internalization of a major tight junction protein, occludin, in macropinosomes (21). Agents that disrupt macropinocytosis interfere with CVB3 entry, as they do with entry of EV1. However, because EV1 entry does not involve any loss of tight junction integrity (we found that the electrical resistance across polarized monolayers does not change during the first 3 h of infection [data not shown]), it is possible that macropinocytosis may serve different functions during entry by EV1 and CVB3.

EV1 entry has previously been examined in two nonpolarized cell lines. In CV-1 monkey kidney cells, virus moves rapidly to caveolin-positive structures within the cell (35); infection appears to involve cholesterol, caveolin, and dynamin, but perturbation of actin dynamics has no effect (35). In SAOS-α2 cells, a human osteosarcoma cell line engineered to express VLA-2, EV1 first enters tubular-vesicular structures within the cytoplasm and ultimately appears in unusual multivesicular bodies, which accumu-

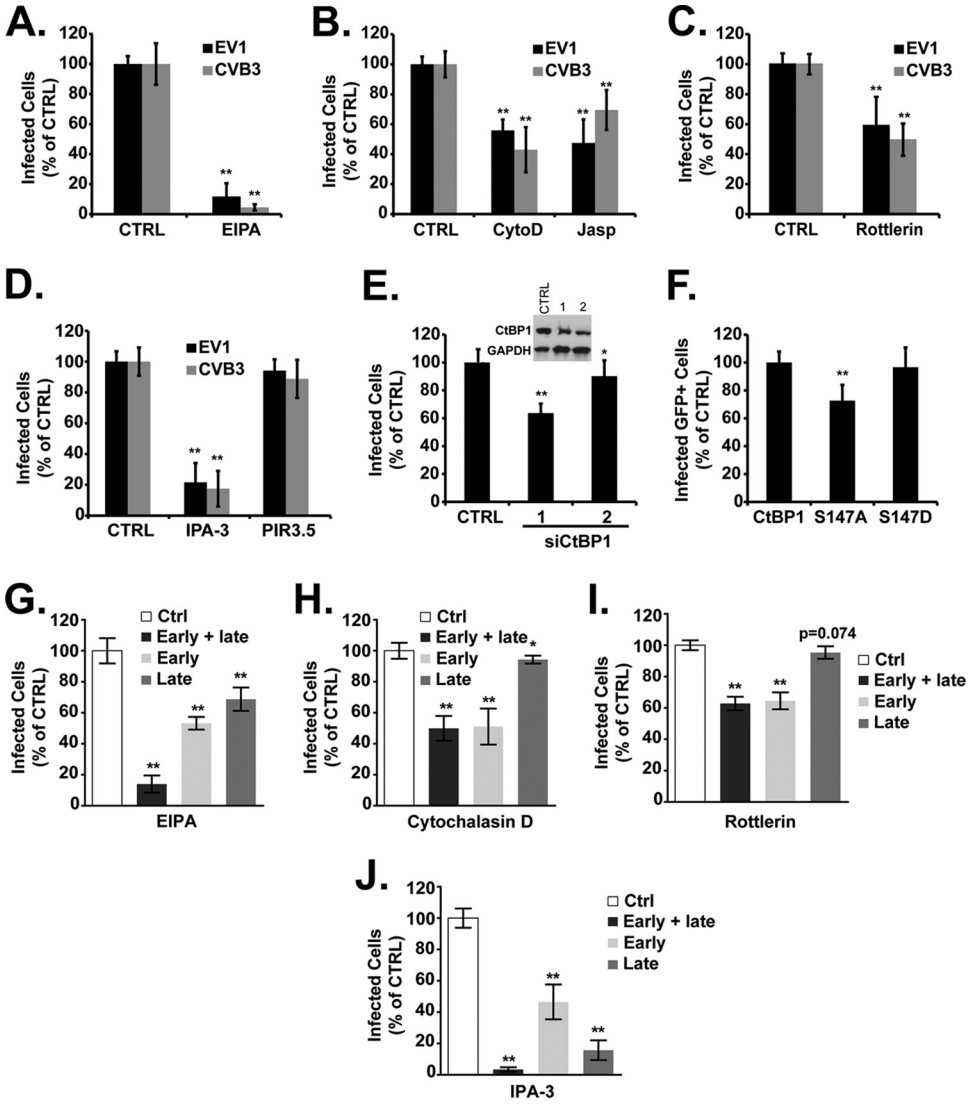

FIG 8 EV1 infection is inhibited by agents that block macropinocytosis. In panels A to D, cells were treated with inhibitors and then infected with EV1 or CVB3 in the presence of inhibitors, as follows: EIPA (A), cytochalasin D (CytoD) or jasplakinolide (Jasp) (B), rottlerin (C), and IPA-3 or PIR3.5 (D). (E) Cells were transfected with two siRNAs targeting CtBP1 (1 and 2). Immunoblot shows silencing of CtBP1. (F) Cells were transfected with plasmids expressing GFP-tagged wild-type CtBP1 or dominant negative CtBP1 (S147A) or a constitutively active form of CtBP1 (S147D) and infected with EV1; results were normalized to those obtained for control cells expressing WT CTBP1. (G to J) Cells were exposed to the indicated drugs throughout infection (early + late), from −1.5 h to 2 h p.i. (early), or from 2 h to 5.5 h p.i. (late). *, $P < 0.05$; **, $P < 0.01$.

late both caveolin and fluid-phase markers (32, 36). Agents that interfere with macropinocytosis inhibit infection of SAOS-α2 cells, either by preventing the internalization of virions (as seen with dominant negative CtBP1) or by preventing traffic to multivesicular bodies (as seen with EIPA) (32, 33). Virus entry into both SAOS-α2 cells and Caco-2 cells may thus involve macropinocytosis. However, the entry pathways in these cell lines appear to differ in some other respects; for example, entry into the osteosarcoma cells, unlike entry into Caco-2 cells, is independent of dynamin. And strikingly, although EV1 moves rapidly to early endosomes in Caco-2 cells, no colocalization between virus and classic endosomal markers is observed during infection in SAOS-α2 cells (14, 32).

The critical final event in picornavirus entry is uncoating, the release of the infectious RNA genome from the capsid. For some picornaviruses, uncoating depends on the low-pH environment encountered within acidified endosomes; for others, uncoating is triggered by contact with the receptor even at neutral pH. We found that EV1 moved rapidly to early endosomes and that infection depended on Rab5, a GTPase involved in early endosome development. Although virus was detected in late endosomes, as determined by colocalization with LAMP-2, infection did not depend on Rab7, a central regulator of late endosome maturation, and was not inhibited by bafilomycin, a drug that prevents endosomal acidification. Thus, it does not appear that virus must traffic through late endosomes before uncoating can occur.

A useful tool for monitoring enterovirus uncoating is the neutral red infectious center assay (37), which is based on the observation that neutral red-loaded virus remains susceptible to inactivation by light until the moment when RNA escapes the capsid.

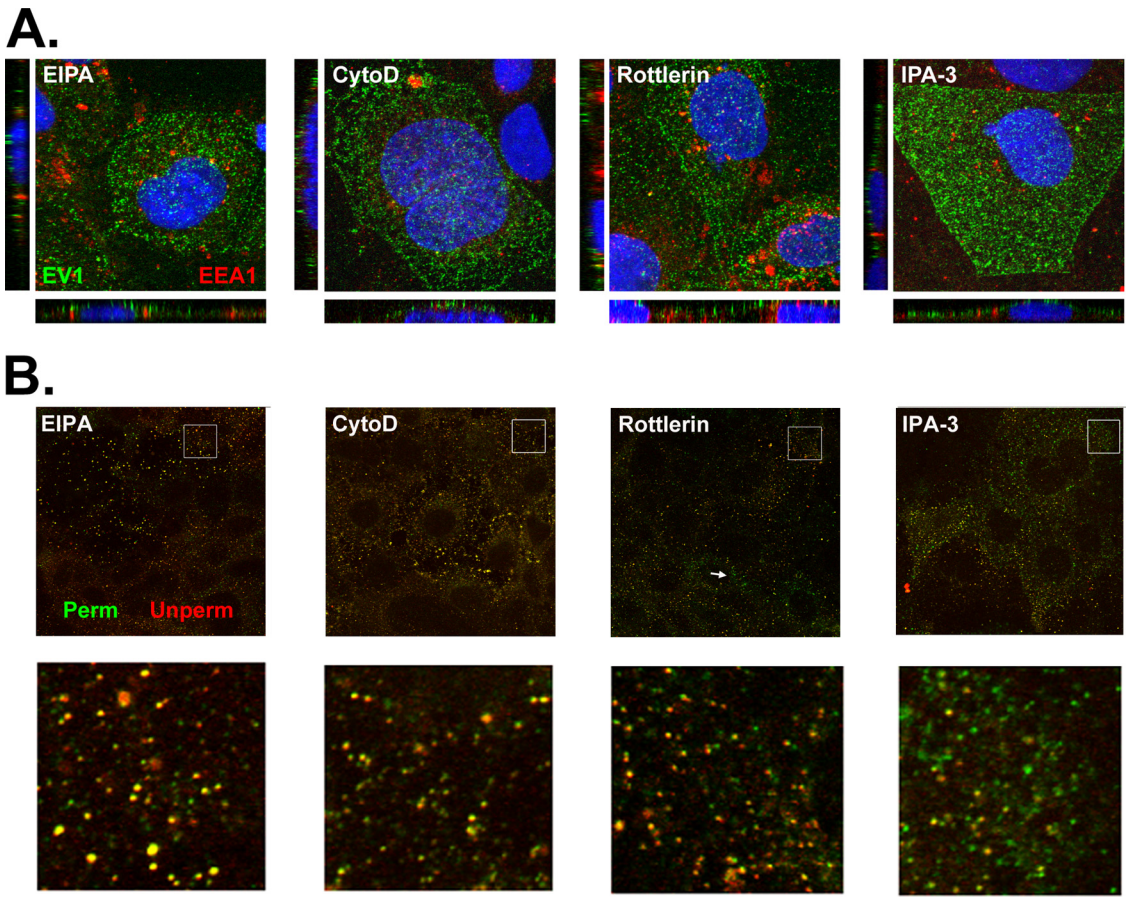

FIG 9 Virus entry depends on factors associated with macropinocytosis. (A) Cells were treated with inhibitors and permitted to bind EV1 (MOI of 200) for 45 min in the cold and then washed and incubated for 30 min at 37°C to permit virus entry; cells were then fixed, permeabilized, and stained with anti-EV1 (green) and anti-EEA1 antibodies (red). (B) Cells treated with inhibitors were infected as described in panel A; at 30 min p.i., cells were fixed, stained with anti-EV1 without permeabilization (Unperm; red), and then refixed, permeabilized, and restained with anti-EV1 (Perm; green). Magnified images of boxed areas are shown in the lower panels.

In applying the neutral red assay to EV1, we found that, as expected, uncoating appeared to be blocked entirely by the uncoating inhibitor R78206 (data not shown). Unexpectedly, however, uncoating was also partially inhibited by brefeldin A, a drug that inhibits infection by other enteroviruses only at postentry steps in replication (11, 37). Although other investigators have suggested that brefeldin inhibits EV1 entry (35), in our hands it does not appear to prevent virus internalization or movement to early en-

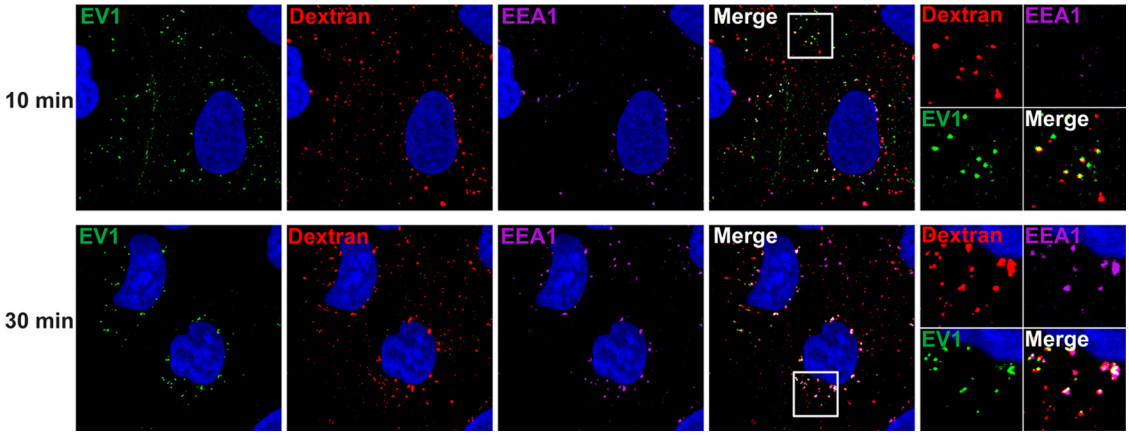

FIG 10 EV1 colocalizes with dextran during entry. Caco-2 cells were incubated with EV1 (MOI of 200) at 4°C to allow virus binding. After 45 min cells were washed with PBS to remove unbound virus. Medium containing 0.1% BSA and 1 mg/ml Texas Red-conjugated dextran (molecular weight, 70,000) was added, and cells were shifted to 37°C to allow virus internalization. After 10 or 30 min cells were extensively washed and fixed. Virus was detected with rabbit anti-EV1 antibody (green), and early endosomes were detected with mouse anti-EEA1 (magenta).

dosomes (data not shown). We do not know whether brefeldin really inhibits infection at another step upstream of RNA release or whether, for some reason, the neutral red assay cannot be used to study EV1. We have not reported results obtained with other inhibitors in the neutral red assay. However, we found that neutral red-loaded EV1 became resistant to light inactivation at 90 min after infection, which may indicate that uncoating does not occur until virus has largely moved from early endosomes to some other location within the cell.

ACKNOWLEDGMENTS

We thank Marc McNiven, Ari Helenius, George Bloom, Craig Roy, Urs Greber, and Alice Dautry-Varsat for plasmids, Ron Harty for VSV, and Douglas Lyles for anti-VSV antibody. Andrea Stout and Jasmine Zhao of the University of Pennsylvania Cell and Developmental Microscopy Core provided assistance with confocal imaging. Carolyn Coyne, Carolina Jaquenod De Giusti, and Yorihiro Nishimura provided helpful comments on the manuscript.

This work was supported by grants from the NIH (R01AI072490) and the Finnish Academy (114727) and by the Plotkin Endowed Chair in Infectious Diseases at Children's Hospital of Philadelphia.

REFERENCES

1. **Pallansch M, Roos R.** 2007. Enteroviruses: poliovirus, coxsackieviruses, echoviruses, and newer enteroviruses, p 839–894. *In* Knipe DM, Howley PM (ed), Fields virology, 5th ed, vol 1. Lippincott Williams and Wilkins, Philadelphia.
2. **Bergelson JM.** 2010. Receptors, p 73–86. *In* Ehrenfeld E, Domingo E, Roos RP (ed), The picornaviruses. ASM Press, Washington, DC.
3. **Levy H, Bostina M, Filman DJ, Hogle JM.** 2010. Cell entry: a biological and structural perspective, p 87–104. *In* Ehrenfeld E, Domingo E, Roos RP (ed), The picornaviruses. ASM Press, Washington, DC.
4. **Mercer J, Schelhaas M, Helenius A.** 2010. Virus entry by endocytosis. Annu. Rev. Biochem. **79:**803–833.
5. **Mercer J, Helenius A.** 2012. Gulping rather than sipping: macropinocytosis as a way of virus entry. Curr. Opin. Microbiol. **15:**490–499.
6. **Yoder JD, Cifuente JO, Pan J, Bergelson JM, Hafenstein S.** 2012. The crystal structure of a coxsackievirus B3-RD variant and a refined 9-angstrom cryo-electron microscopy reconstruction of the virus complexed with decay-accelerating factor (DAF) provide a new footprint of DAF on the virus surface. J. Virol. **86:**12571–12581.
7. **West MA, Bretscher MS, Watts C.** 1989. Distinct endocytotic pathways in epidermal growth factor-stimulated human carcinoma A431 cells. J. Cell Biol. **109:**2731–2739.
8. **Schleissner LA, Portnoy B.** 1973. Spectrum of ECHO virus 1 disease in a young diabetic. Chest **63:**457–459.
9. **Rousset M.** 1986. The human colon carcinoma cell lines HT-29 and Caco-2: two in vitro models for the study of intestinal differentiation. Biochimie **68:**1035–1040.
10. **Bergelson JM, Shepley MP, Chan BMC, Hemler ME, Finberg RW.** 1992. Identification of the integrin VLA-2 as a receptor for echovirus 1. Science **255:**1718–1720.
11. **Kim C, Bergelson JM.** 2012. Echovirus 7 entry into polarized intestinal epithelial cells requires clathrin and Rab7. mBio **3**(2):e00304–11. doi:10.1128/mBio.00304-11.
12. **Coyne CB, Bergelson JM.** 2006. Virus-induced Abl and Fyn kinase signals permit coxsackievirus entry through epithelial tight junctions. Cell **124:**119–131.
13. **Patel KP, Coyne CB, Bergelson JM.** 2009. Dynamin- and lipid raft-dependent entry of decay-accelerating factor (DAF)-binding and non-DAF-binding coxsackieviruses into nonpolarized cells. J. Virol. **83:**11064–11077.
14. **Marjomaki V, Pietiainen V, Matilainen H, Upla P, Ivaska J, Nissinen L, Reunanen H, Huttunen P, Hyypia T, Heino J.** 2002. Internalization of echovirus 1 in caveolae. J. Virol. **76:**1856–1865.
15. **Cao H, Thompson HM, Krueger EW, McNiven MA.** 2000. Disruption of Golgi structure and function in mammalian cells expressing a mutant dynamin. J. Cell Sci. **113:**1993–2002.
16. **Pelkmans L, Kartenbeck J, Helenius A.** 2001. Caveolar endocytosis of simian virus 40 reveals a new two-step vesicular-transport pathway to the ER. Nat. Cell Biol. **3:**473–483.
17. **Benmerah A, Lamaze C, Bègue B, Schmid SL, Dautry-Varsat A, Cerf-Bensussan N.** 1998. AP-2/Eps15 interaction is required for receptor-mediated endocytosis. J. Cell Biol. **140:**1055–1062.
18. **Amstutz B, Gastaldelli M, Kalin S, Imelli N, Boucke K, Wandeler E, Mercer J, Hemmi S, Greber UF.** 2008. Subversion of CtBP1-controlled macropinocytosis by human adenovirus serotype 3. EMBO J. **27:**956–969.
19. **Coyne CB, Voelker T, Pichla SL, Bergelson JM.** 2004. The coxsackievirus and adenovirus receptor interacts with the multi-PDZ domain protein-1 (MUPP-1) within the tight junction. J. Biol. Chem. **279:**48079–48084.
20. **Elices MJ, Hemler ME.** 1989. The human integrin VLA-2 is a collagen receptor on some cells and a collagen-laminin receptor on others. Proc. Natl. Acad. Sci. U. S. A. **86:**9906–9910.
21. **Coyne CB, Shen L, Turner JR, Bergelson JM.** 2007. Coxsackievirus entry from epithelial tight junctions requires occludin and the small GTPases Rab34 and Rab5. Cell Host Microbe **2:**181–192.
22. **Macia E, Ehrlich M, Massol R, Boucrot E, Brunner C, Kirchhausen T.** 2006. Dynasore, a cell-permeable inhibitor of dynamin. Dev. Cell **10:**839–850.
23. **Arthur JR, Heinecke KA, Seyfried TN.** 2011. Filipin recognizes both GM1 and cholesterol in GM1 gangliosidosis mouse brain. J. Lipid Res. **52:**1345–1351.
24. **Ivanov AI.** 2008. Pharmacological inhibition of endocytic pathways: is it specific enough to be useful? Methods Mol. Biol. **440:**15–33.
25. **Awasthi-Kalia M, Schnetkamp PP, Deans JP.** 2001. Differential effects of filipin and methyl-beta-cyclodextrin on B cell receptor signaling. Biochem. Biophys. Res. Commun. **287:**77–82.
26. **Haspot F, Lavault A, Sinzger C, Laib Sampaio K, Stierhof YD, Pilet P, Bressolette-Bodin C, Halary F.** 2012. Human cytomegalovirus entry into dendritic cells occurs via a macropinocytosis-like pathway in a pH-independent and cholesterol-dependent manner. PLoS One **7:**e34795. doi:10.1371/journal.pone.0034795.
27. **Torgersen ML, Skretting G, van Deurs B, Sandvig K.** 2001. Internalization of cholera toxin by different endocytic mechanisms. J. Cell Sci. **114:**3737–3747.
28. **Sun X, Yau VK, Briggs BJ, Whittaker GR.** 2005. Role of clathrin-mediated endocytosis during vesicular stomatitis virus entry into host cells. Virology **338:**53–60.
29. **Cureton DK, Massol RH, Saffarian S, Kirchhausen TL, Whelan SP.** 2009. Vesicular stomatitis virus enters cells through vesicles incompletely coated with clathrin that depend upon actin for internalization. PLoS Pathog. **5:**e1000394. doi:10.1371/journal.ppat.1000394.
30. **Somsel Rodman J, Wandinger-Ness A.** 2000. Rab GTPases coordinate endocytosis. J. Cell Sci. **113:**183–192.
31. **Matlin KS, Reggio H, Helenius A, Simons K.** 1982. Pathway of vesicular stomatitis virus entry leading to infection. J. Mol. Biol. **156:**609–631.
32. **Karjalainen M, Kakkonen E, Upla P, Paloranta H, Kankaanpaa P, Liberali P, Renkema GH, Hyypia T, Heino J, Marjomaki V.** 2008. A Raft-derived, Pak1-regulated entry participates in α2β1 integrin-dependent sorting to caveosomes. Mol. Biol. Cell **19:**2857–2869.
33. **Liberali P, Kakkonen E, Turacchio G, Valente C, Spaar A, Perinetti G, Bockmann RA, Corda D, Colanzi A, Marjomaki V, Luini A.** 2008. The closure of Pak1-dependent macropinosomes requires the phosphorylation of CtBP1/BARS. EMBO J. **27:**970–981.
34. **Sarkar K, Kruhlak MJ, Erlandsen SL, Shaw S.** 2005. Selective inhibition by rottlerin of macropinocytosis in monocyte-derived dendritic cells. Immunology **116:**513–524.
35. **Pietiainen V, Marjomaki V, Upla P, Pelkmans L, Helenius A, Hyypia T.** 2004. Echovirus 1 endocytosis into caveosomes requires lipid rafts, dynamin II, and signaling events. Mol. Biol. Cell **15:**4911–4925.
36. **Karjalainen M, Rintanen N, Lehkonen M, Kallio K, Maki A, Hellstrom K, Siljamaki V, Upla P, Marjomaki V.** 2011. Echovirus 1 infection depends on biogenesis of novel multivesicular bodies. Cell Microbiol. **13:**1975–1995.
37. **Brandenburg B, Lee LY, Lakadamyali M, Rust MJ, Zhuang X, Hogle JM.** 2007. Imaging poliovirus entry in live cells. PLoS Biol. **5:**e183. doi:10.1371/journal.pbio.0050183.